A Novel Prescribed-Time Control Approach of State-Constrained High-Order Nonlinear Systems

Yangang Yao, Yu Kang, Yunbo Zhao, Pengfei Li, and Jieqing Tan

***Abstract*—A novel practical prescribed-time control (PPTC) approach for high-order nonlinear systems (HONSs) subject to state constraints is studied in this article. Different from the existing methods which always require the constraint boundaries to be continuous functions, the state constraints considered in this article are discontinuous (i.e., the state constraints occur only in some time periods and not in others), which can be found in many practical systems. By designing a novel stretch model-based nonlinear mapping function (NMF), the state constraints are dealt with directly, and the limitations that the virtual control function depends upon the feasibility condition (FC) and the tracking error depends upon the constraint boundaries in the conventional schemes are removed. Meanwhile, the proposed method is a unified one, which is also effective for HONSs with conventional continuous state constraints/ deferred state constraints/ funnel constraints or constraints-free without altering the control structure. Furthermore, by designing a newly time-varying scaling transformation function (STF), a more relaxed criterion for practical prescribed-time stable (PPTS) is given, based on which a newly PPTC algorithm is designed. The result shows that the proposed algorithm can preset the upper bound of the settling time, which does not depend upon the initial state of the system and control parameters, the limitations of singularity problem and excessive initial control input in existing methods are removed. Simulation examples verify the algorithm developed.**

***Index Terms*—Fuzzy control, high-order nonlinear systems, practical prescribed-time control (PPTC), state constraints.**

I. Introduction

IN VIEW of production safety or control performance, adaptive control of nonlinear systems subject to state constraints has become a hot topic in the past few decades. Early schemes include set invariance notions [1], reference governors [2], and model predictive control [3]. Regrettably, the above schemes depend on computationally intensive algorithms. To this end, an effective tool called barrier Lyapunov function (BLF) was presented in [4], which can deal with state constraints without depending on computationally intensive algorithms. Afterwards, many significant BLF-based algorithms were obtained for state/output-constrained systems, see [5], [6], [7] and related references. However, the core of BLF-based approach is to transform the state constraints into error constraints. Since the tracking error involves the virtual control function, the BLF-based method has an obvious limitation that the virtual control function should always be within the constraint range, i.e., the so called "FC." Subsequently, some nonlinear mapping function (NMF)-based schemes were proposed by introducing the NMF that only contain state variables [8], [9], [10], [11], [12], which can effectively remove the feasibility condition (FC). It is noteworthy that the schemes proposed in [4], [5], [6], [7], [8], [9], [10], [11], and [12] are aimed at general feedback nonlinear systems subject to state/output constraints, and are not suitable for high-order nonlinear systems (HONSs).

Since there is at least one p_i greater than 1, the Jacobian linearization of HONSs (see (1)) may not be controllable and feedback linearizable, the control of state-constrained HONSs is bound to be more trickier. Even so, some remarkable progresses were achieved in recent years [13], [14], [15], [16], [17], [18]. For example, by virtue of designing the log-type high-order BLF (L-HBLF), two newly control algorithms for full-state constrained HONSs were obtained in [13] and [14]. The unified methods based on tan-type high-order BLF (T-HBLF) were presented for HONSs with state constraints [15], [16], which are still effective for HONSs without constraints. Similar to the BLF-based methods [5], [6], [7], the L/T-HBLF-based methods also have the disadvantage of relying on FC. To this end, the NMF-based schemes of state-constrained HONSs were presented [17], [18], [19], [20]. To name a list, inspired by the ideas in [8], the asymptotic tracking [17] and practical tracking control [18] were presented for HONSs with state constraints. Yao et al. [19] proposed a novel fuzzy control of HONSs with multitype state constraints, which can be applied to HONSs with different constrained boundaries without changing the control structure. Recently, a unified scheme for full-state constrained stochastic HONSs was presented in [20], a significant advantage is that the tracking error no longer depends on constraint boundaries. It is particularly worth emphasizing that all the methods mentioned above assume that the constraint boundaries are continuous, which means

Manuscript received 30 August 2023; accepted 9 January 2024. This work was supported in part by the National Key Research and Development Program of China under Grant 2018AAA0100801, and in part by the National Natural Science Foundation of China under Grant 62033012, Grant 62103394, Grant 62173317, Grant 61725304, and Grant 62172135. This article was recommended by Associate Editor X. Su. *(Corresponding author: Yu Kang.)*

Yangang Yao is with the School of Information and Artificial Intelligence, Anhui Agricultural University, Hefei 230036, China, and also with the Department of Automation, University of Science and Technology of China, Hefei 230027, China (e-mail: ygyao@ustc.edu.cn).

Yu Kang, Yunbo Zhao, and Pengfei Li are with the Department of Automation, University of Science and Technology of China, Hefei 230027, China (e-mail: kangduyu@ustc.edu.cn; ybzhao@ustc.edu.cn; puffylee@ustc.edu.cn).

Jieqing Tan is with the School of Mathematics, Hefei University of Technology, Hefei 230601, China (e-mail: jieqingtan@hfut.edu.cn).

Color versions of one or more figures in this article are available at https://doi.org/10.1109/TSMC.2024.3352905.

Digital Object Identifier 10.1109/TSMC.2024.3352905

that the state constraints always exist. Nevertheless, many actual systems usually encounter state constraints only in some special time periods, and not in other time periods. To take a simple example, an unmanned robot needs to travel through multiple narrow areas to carry out a rescue mission, in fact, the robot only encounters constraints in certain narrow areas and task execution areas, but not in other time intervals (hereinafter referred to as "intermittent state constraints"). Obviously, this involves multiple alternating between constrained and unconstrained cases. Although the T-HBLF-based methods [15], [16] and NMF-based method [19], [20] are also suitable for unconstrained HONSs, they still cannot deal with the intermittent state constraints that alternate between constrained and unconstrained. Therefore, it is a meaningful and challenging work to investigate the control scheme for HONSs with intermittent state constraints.

In addition, the settling time is also a particularly important consideration in practical system control, and usually a finite and controllable settling time is favored by users. To this end, many finite-time control (FTC) methods were obtained for output/state-constrained HONSs [21], [22], [23], [24]. Bearing in mind that the settling time of FTC algorithms depends upon the initial state of the system. Another FTC methods based on finite-time prescribed performance function (FTPPF) were proposed in [25], [26], [27], and [28]. The disadvantage of these methods is that variable transformation is required, which increases the computational complexity to some extent. Then, the fixed-time control (FxTC) algorithms were presented for general feedback nonlinear systems [29], [30] and HONSs [19], [20], [31], [32], which effectively removes the limitation that the settling time depends upon the initial value. Although the FxTC has a significant advantage over the FTC, it still has some limitations, like the upper bound of the settling time of theoretical analysis differs greatly from the simulation results, and the relationship between the upper bound and design parameters is ambiguous [33].

Recently, prescribed-time control (PTC) have attracted a lot of attention, which has a prominent advantage that the settling time can be preset. It is very valuable for the control of many practical systems (such as UAV for intensive rescue, military targeted attacks, and so on), and a large number of effective PTC methods were proposed. To name a list, by designing the scaling transformation function (STF), the PTC schemes were presented for uncertain nonlinear systems [35], [36], switched nonlinear systems [37], multiagent systems [38], stochastic nonlinear systems [39], [40] and HONSs [41]. It is worthy noting that the STF designed in [35], [36], [37], [38], [39], [40], and [41] goes to infinity as time tends to the prescribed terminal time, which might cause a singularity problem in implementing the constructed controller. Toward this end, Ning et al. [42] presented a practical prescribed-time control (PPTC) algorithm by designing a time base generator. Recently, Guo and Hu [43] applied this method to HONSs. However, the above methods follow $\dot{V} \leq -\kappa(t)V$ when designing the controller (where V denotes the Lyapunov function (LF), $\kappa(t)$ denotes a time-varying function of time-based generator), which is undoubtedly very demanding. Then, some new PPTC methods based on more relaxed conditions were proposed in [44], [45], [46], and [47]. For instance, two event-triggered-based PPTC methods were presented for space teleoperation systems [44] and state-constrained nonlinear systems [45]. One drawback of the above methods is that the designed controller is prone to singularity. Two PPTC methods were proposed for interconnected systems [46] and strict-feedback nonlinear systems [47], where the LF V needs to be satisfied $\dot{V} \leq (\pi/(rT))(V^{1+r/2} + V^{1-r/2}) + \varrho$ (where $r \in (0, 1)$, T and ϱ are positive constants). Since the designed control input contains a term with a power greater than one, so that when the initial state deviates from the equilibrium point by a large amount, the initial control input becomes large. Recently, Zou et al. [48] proposed a new PPTC scheme, which can effectively overcome the problems of singularity and large initial control input. Nevertheless, the method presented in [48] is only suitable for general feedback nonlinear systems without state constraints, which leads us to study a novel PPTC algorithm for intermittent state-constrained HONSs.

To sum up, although the remarkable progresses have been made for control of state-constrained HONSs, there are still some limitations.

1) The existing methods to deal with state constraints are mainly divided into two categories, i.e., T/L-HBLF-based methods [13], [14], [15], [16] and NMF-based methods [17], [18], [19], [20]. The former depends on the FC, although the latter removes the FC, while they are only applicable to continuous state-constrained HONSs, but not to the intermittent state-constrained HONSs.
2) The existing control algorithms of HONSs can only ensure finite/fixed-time stability except for those in [41] and [43].

However, the STF designed in [41] goes to infinity as time tends to the prescribed terminal time, which might cause a singularity problem in implementing the constructed controller, and the PPTC method proposed in [43] follow $\dot{V} \leq -\kappa(t)V$ when designing the controller, which is undoubtedly very demanding. As far as we know, the PPTC scheme of HONSs with intermittent state constraints has not made progress. Therefore, this article attempts to take a step forward toward addressing such a challenging problem. The contributions are concluded as follows.

1) Distinct from the conventional control methods of state-constrained HONSs [13], [14], [15], [16], [17], [18], [19], [20],which are only applicable to HONSs with continuous constrained boundaries. The intermittent state constraint considered in this article is characterized by constraint discontinuity, which means that the state constraints occur only in some time periods and not in others. By designing a novel stretch model-based NMF, the intermittent state constraints are handled, and the limitations of virtual control function depends upon FC [13], [14], [15], [16] and tracking error depends upon constraint boundaries are removed [17], [18], [19]. Moreover, the proposed method is a unified scheme, which is also applicable to HONSs with conventional continuous state constraints/deferred state constraints/funnel constraints or constraints-free without changing the control structure.

2) With the aid of a newly smooth STF, a novel criterion for practical prescribed-time stable (PPTS) is given, which is more relaxed than that in [42] and [43]. Combined with FLS and backstepping technique, a newly PPTC algorithm for intermittent state constrained HONSs is designed. The proposed algorithm can preset the upper bound of the settling time, which does not depend upon the initial state of the system and control parameters, and the limitations of the singularity problem in [35], [36], [37], [38], [39], [40], [41], [44], and [45] and the excessive initial control input in [46] and [47] are removed.

II. Problem Formulation and Preliminaries

A. Problem Formulation

This article considers a class of uncertain HONSs

$$\begin{cases} \dot{x}_i = f_i(\bar{x}_i) + g_i(\bar{x}_i)x_{i+1}^{p_i}, i = 1, \ldots, n-1 \\ \dot{x}_n = f_n(\bar{x}_n) + g_n(\bar{x}_n)u^{p_n} \\ y = x_1 \end{cases} \tag{1}$$

and the following state constraints need to be observed:

$$x \in \mathscr{B}_x = \left\{ x \in R^n \middle| y_d - L_1(t) < x_1 < y_d + H_1(t) \right. \\ \left. - L_i(t) < x_i < H_i(t) \quad \forall t \in \left[t_{s,j}^i, t_{e,j}^i\right] \right\} \tag{2}$$

where $i = 2, \ldots, n$, $\bar{x}_n = [x_1, \ldots, x_n]^T$ denotes system state, and $\bar{x}_i = [x_1, \ldots, x_i]^T$. y, u represent system output and input, respectively. $f_i(\cdot)$ and $g_i(\cdot)$ represent uncertain continuous nonlinear function with $i = 1, \ldots, n$. $p_i \in R_{\text{odd}}^{\geq 1} = \{q_1/q_2 | q_i$ denotes a positive odd constant,$q_1 > q_2\}$. The differentiable constraint boundaries $-L_i(t)$ and $H_i(t)$ satisfy $-L_i(t) < 0 < H_i(t)$. $[t_{s,j}^i, t_{e,j}^i]$ represents the jth constraint interval of x_i, satisfying $0 \leq t_{s,j}^i \leq t_{e,j}^i \leq t_{s,j+1}^i \leq t_{e,j+1}^i \leq \infty$ with $j = 1, \ldots, k^i - 1$.

Remark 1: It is worth noting that the state constraint considered in this article is discontinuous, which means that the state variable x_i is constrained in k^i time intervals, but not in other intervals, i.e., $x_i \in (-L_i(t), H_i(t))$ for $\forall t \in [t_{s,j}^i, t_{e,j}^i]$, $j = 1, \ldots, k^i, i = 1, \ldots, n$, and in other time intervals, the system has no state constraints. Obviously, the control design of HONSs with intermittent state constraints is not straight forward. Moreover, the proposed scheme is also suitable for HONSs with conventional continuous state constraints/deferred constraints/funnel constraints or constraints-free without changing the control structure (see Remark 9).

This article aims to construct an effective control algorithm to ensure that all signals of HONS (1) are semi-global bounded, and the intermittent state constraints are not violated, i.e., $x \in \mathscr{B}_x$. Meanwhile, the system output y tracks the given desired signal y_d within a prescribed time.

To achieve the control objectives, two rationalization assumptions are given as follows.

Assumption 1 [19]: The first derivative of the desired signal y_d is bounded and continuous.

Assumption 2 [20]: $g_i(\cdot)$ is strictly positive or strictly negative bounded function, and $\exists\ \underline{g} \in R^+$, such that $0 < \underline{g} \leq |g_i(\cdot)| < +\infty$. For the sake of simplicity, let $g_i(\cdot) > 0$.

Remark 2: Assumptions 1-2 are two reasonable assumptions used for control of nonlinear systems that widely exist in many literatures. Of course, when the control direction is unknown (i.e., the sign of $g(\cdot)$ is unknown), there are already some effective processing schemes, see [49] for details. Since this article focuses on the PPTC of state-constrained HONSs, the proposed scheme is carried out under Assumption 2 for analysis simplicity, and the same assumption is also given in [19] and [20]. In fact, many actual systems do satisfy Assumption 2, like single-link manipulator system, the permanent magnet brush dc motor system, and so on.

B. Practical Prescribed-Time Stable

Definition 1 [48]: For the following system:

$$\dot{x} = f(x, t), f(\mathbf{0}, t) = 0 \tag{3}$$

where $f : R^m \times R^+ \to R^m$ denotes a nonlinear continuous function. Let $x = \mathbf{0}$ be the solution of system (3). If $\exists\ T \in R^+$ such that

$$x(t) = \mathbf{0} \quad \forall t \in [T, +\infty) \tag{4}$$

then, the solution of (3) is PTS. If $\exists\ \epsilon \in R^+, T \in R^+$ such that

$$\|x(t)\| \leq \epsilon \quad \forall t \in [T, +\infty) \tag{5}$$

then, the solution of (3) is PPTS.

First, a novel STF $\kappa(t)$ is designed as follows:

$$\kappa(t) = \begin{cases} \frac{1}{\varepsilon + (1 - \frac{t}{T})^n}, & t \in [0, T] \\ \frac{1}{\varepsilon}, & t \in (T, +\infty) \end{cases} \tag{6}$$

where T and ε are positive design parameters, and $0 < \varepsilon \ll 1$. Obviously, $\kappa(t)$ has the following properties.

1) $\kappa(t)$ is nondecreasing and continuous on $[0, +\infty)$, and $\kappa(0) = 1/(1 + \varepsilon)$, $\kappa(T) = 1/\varepsilon$.
2) $\kappa(t)$ is C^n on $[0, +\infty)$.

Next, a sufficient condition for the PPTS of system (3) will be shown by Lemma 1.

Lemma 1: Given a radially unbounded positive definite LF $V(t)$, if $\exists\ c, \varrho \in R^+$, such that

$$\dot{V}(t) \leq -cV(t) - \frac{\dot{\kappa}(t)}{\kappa(t)}V(t) + \varrho \tag{7}$$

then, one has $V(t) \leq \varepsilon V(0) + \varrho/c$ when $t \geq T$, and $V(t) \to \varrho/c$ as $t \to +\infty$.

Proof: Let $\bar{V}(t) = \kappa(t)V(t)$, then one can obtain

$$\dot{\bar{V}}(t) \leq -c\bar{V}(t) + \kappa(t)\varrho. \tag{8}$$

Based on (8), one has

$$\bar{V}(t) \leq \frac{V(0)e^{-t}}{1 + \varepsilon} + \frac{\varrho}{c\varepsilon}. \tag{9}$$

Then, we can further obtain

$$V(t) \leq \frac{V(0)e^{-t}}{(1 + \varepsilon)\kappa(t)} + \frac{\varrho}{c\varepsilon\kappa(t)}. \tag{10}$$

It can be seen from (10) that $V(t) \leq \varepsilon V(0) + \varrho/c$ when $t \geq T$, and $V(t) \to \varrho/c$ as $t \to +\infty$. ∎

Remark 3: It is noted that when $\varrho = 0$, one has $V(t) \leq \varepsilon V(0)$ when $t \geq T$, and then asymptotically converges to 0, the proposed scheme can degenerate to the results in [42] and [43]. For PTC methods in [39] and [40], the STF is designed as $\kappa(t) = T/(T-t)$, so $\kappa(t)$ goes to infinity as time tends to the prescribed time T, which obviously cause a singularity problem in implementing the designed controller. However, the novel STF (6) constructed in this article is C^n on $[0, +\infty)$, the singularity problem is avoided.

Remark 4: The sufficient condition for the PPTS given in [42] and [43] is that the LF V needs to be satisfied $\dot{V} \leq -\kappa_1(t)V$, where $\kappa_1(t)$ denotes a positive function, including the time-based generator. Obviously, this condition is undoubtedly very demanding, and does not apply to the control of HONSs where the system functions are completely unknown. The sufficient condition for the PPTS given in [44] and [45] is that the LF V needs to be satisfied $\dot{V} \leq -cV - (2\dot{\kappa}_2(t)/\kappa_2(t))V + \eta/\kappa_2(t) + \varrho$, where $\kappa_2(t)$ denotes a time-varying piecewise function, $c, \eta, \varrho \in R^+$. The term $\eta/\kappa_2(t)$ on the right-hand side of the inequality makes the designed controller prone to singularity problems. The sufficient condition for the PPTS given in [46] and [47] is that V should be satisfied $\dot{V} \leq (\pi/(rT))(V^{1+r/2} + V^{1-r/2}) + \varrho$ (where $r \in (0,1)$, T and ϱ are positive constants), under which the designed control input contains a term with a power greater than one, so that when the initial state deviates from the equilibrium point by a large amount, an excessive initial control input may occur. Obviously, it can be seen from Lemma 1 that the above limitations are overcome in this article. Compared with the FTPPF-based FTC algorithm [25], [26], [27], [28], the proposed PPTC algorithm does not require any state transition, so the control design process is simpler.

C. Important Lemmas

Lemma 2 [13]: For an unknown nonlinear function $\mathscr{F}(\mathbb{Z})$, a FLS can be used to approximate it in the following form:

$$\mathscr{F}(\mathbb{Z}) = \Delta(\mathbb{Z}) + \Upsilon^T \Pi(\mathbb{Z}), \quad \left(|\Delta(\mathbb{Z})| \leq \Delta, \Delta \in R^+\right) \tag{11}$$

where $\Pi(\mathbb{Z}), \Upsilon, \mathbb{Z}, \Delta(\mathbb{Z})$ denote basis function, weight, input and error, respectively.

$$\Pi(\mathbb{Z}) = \frac{[\Pi_1(\mathbb{Z}), \ldots, \Pi_m(\mathbb{Z})]^T}{\sum_{i=1}^n \Pi_i(\mathbb{Z})}, m \in R^+$$

with

$$\Pi_i(\mathbb{Z}) = \exp\left[\frac{-(\mathbb{Z} - \mathcal{Z}_i)^T(\mathbb{Z} - \mathcal{Z}_i)}{\iota_i{}^2}\right], i = 1, \ldots, m.$$

$\mathcal{Z}_i$ and ι_i are the center vector and the spreads of $\Pi_i(\mathbb{Z})$.

Lemma 3 [19]: For $\alpha, \beta, \gamma \in R^+$, $\phi, \psi \in R$, $p \in R^{\geq 1}_{\text{odd}}$, one has

$$|\phi|^\alpha |\psi|^\beta \leq \frac{\gamma\alpha}{\alpha+\beta}|\phi|^{\alpha+\beta} + \frac{\beta\gamma^{-\frac{\alpha}{\beta}}}{\alpha+\beta}|\psi|^{\alpha+\beta} \tag{12}$$

$$|\phi^p - \psi^p| \leq \Xi|\phi - \psi|\Big(|\phi - \psi|^{p-1} + |\psi|^{p-1}\Big) \tag{13}$$

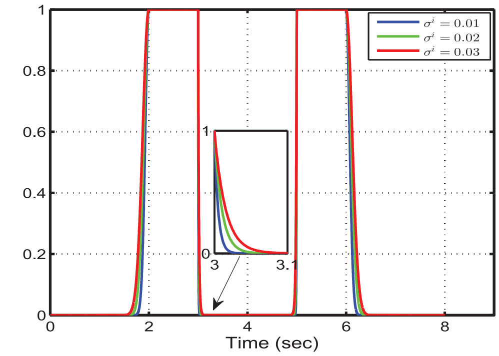

Fig. 1. Graphs of $\mathscr{S}_i(t)$ with $\sigma^i = 0.01, 0.02.0.03$.

where $\Xi = p(2^{p-2} + 2)$.

Lemma 4 [20]: For $\phi \geq 0$, $\psi > 0$ and $\gamma \geq 1$, one has

$$\phi \leq \psi + \left(\frac{\phi}{\gamma}\right)^\gamma \left(\frac{\gamma-1}{\psi}\right)^{\gamma-1}. \tag{14}$$

III. Main Results

A. System Transformation

Design a stretching function as follows:

$$\mathscr{S}_i(t) = \begin{cases} e^{\Gamma_1^i(t)}, & t \in [0, t_{s,1}^i) \\ 1, & t \in [t_{s,j}^i, t_{e,j}^i), j = 1, \ldots, k^i \\ e^{\Gamma_{j+1}^i(t)}, & t \in [t_{e,j}^i, t_{s,j+1}^i), j = 1, \ldots, k^i - 1 \\ e^{\Gamma_{k^i+1}^i(t)}, & t \in [t_{e,k^i}^i, +\infty) \end{cases} \tag{15}$$

where $i = 1, \ldots, n$, and

$$\Gamma_1^i(t) = -\frac{\left(t - t_{s,1}^i\right)^{2n}}{\sigma_1^i}, \Gamma_{k^i+1}^i(t) = -\frac{\left(t_{e,k^i}^i - t\right)^{2n}}{\sigma_{k^i+1}^i}$$

$$\Gamma_{j+1}^i(t) = \frac{\left(t - \frac{t_{e,j}^i + t_{s,j+1}^i}{2}\right)^{2n} - \left(\frac{t_{e,j}^i - t_{s,j+1}^i}{2}\right)^{2n}}{\sigma_{j+1}^i}$$

with $j = 1, \ldots, k^i - 1$, and $0 < \sigma_j^i \ll 1$ denotes the design parameter. Obviously, the smaller σ_j^i, the faster $\mathscr{S}_i(t)$ converges at the piecewise point. Fig. 1 shows the graphs of $\mathscr{S}_i(t)$ when $\sigma^i = 0.01, 0.02.0.03$, respectively, where $t_{s,1}^i = 2$, $t_{e,1}^i = 3$, $t_{s,2}^i = 5$, $t_{e,2}^i = 6$.

According to Fig. 1 and (15), one can know that $\mathscr{S}_i(t)$ has the following properties.

1) $\mathscr{S}_i(t) \equiv 1$ for $\forall t \in [t_{s,j}^i, t_{e,j}^i]$, and $\lim_{t \to t_{s,j}^{i}{}^-} \mathscr{S}_i(t) = \lim_{t \to t_{e,j}^{i}{}^+} \mathscr{S}_i(t) = 1$.
2) $\mathscr{S}_i(t)$ approaches 0 on the large measure subset of $(0, t_{s,1}^i) \cup \ldots (t_{e,j}^i, t_{s,j+1}^i) \ldots \cup (t_{e,k^i}^i, +\infty)$, $j = 1, \ldots, k^i - 1$.
3) $\mathscr{S}_i(t)$ is continuous on $t \in [0, +\infty)$.

The following auxiliary variables are introduced:

$$\begin{cases} \eta_1(t) = e_1 \mathscr{S}_1(t) \\ \eta_i(t) = x_i \mathscr{S}_i(t), i = 2, \ldots, n \end{cases} \tag{16}$$

where $e_1 = x_1 - y_d$ denotes the tracking error.

Inspired by [20], the following C^n functions are designed:

$$\hbar_{i1}(\eta_i(t), L_i(t)) = -\mathscr{N}_i(\eta_i(t))\left(\frac{\eta_i(t)}{L_i(t)}\right)^{2m} + 1 \tag{17}$$

$$\hbar_{i2}(\eta_i(t), H_i(t)) = -\bar{\mathscr{N}}_i(\eta_i(t))\left(\frac{\eta_i(t)}{H_i(t)}\right)^{2m} + 1 \tag{18}$$

where $2m > n, m \in z^+$, $\bar{\mathscr{N}}_i(\eta_i(t)) = 1 - \mathscr{N}_i(\eta_i(t))$, and

$$\mathscr{N}_i(\eta_i(t)) = \begin{cases} 1, & -L_i(t) < \eta_i(t) \le 0 \\ 0, & 0 < \eta_i(t) < H_i(t). \end{cases}$$

For simplicity, in the remainder of this article, let $L_i = L_i(t), H_i = H_i(t), \eta_i = \eta_i(t), \hbar_{i1} = \hbar_{i1}(\eta_i, L_i), \hbar_{i2} = \hbar_{i2}(\eta_i, H_i), \mathscr{S}_i = \mathscr{S}_i(t), \mathscr{N}_i = \mathscr{N}_i(\eta_i), \bar{\mathscr{N}}_i = \bar{\mathscr{N}}_i(\eta_i(t))$ with $i = 1, \ldots, n$.

Then, perform the following NMF:

$$\begin{cases} \chi_1 = \frac{e_1}{\hbar_{11}\hbar_{12}} \\ \chi_i = \frac{x_i}{\hbar_{i1}\hbar_{i2}}, i = 2, \ldots, n. \end{cases} \tag{19}$$

Based on (17)–(19), it can be known that if $-L_i(0) < \eta_i(0) < H_i(0)$, then $\chi_i \to \infty$ if and only if $\eta_i(t) \to H_i^-(t)$ or $\eta_i(t) \to -L_i^+(t)$. As χ_i is continuous, it can be further obtained that as long as $-L_i(0) < \eta_i(0) < H_i(0)$ and χ_i is bounded, then one has

$$-L_i(t) < \eta_i(t) < H_i(t). \tag{20}$$

Based on (16) and (20), we can further obtain

$$\begin{cases} \frac{-L_1(t)}{\mathscr{S}_1(t)} < e_1 < \frac{H_1(t)}{\mathscr{S}_1(t)} \\ \frac{-L_i(t)}{\mathscr{S}_i(t)} < x_i < \frac{H_i(t)}{\mathscr{S}_i(t)}, i = 2, \ldots, n. \end{cases} \tag{21}$$

Remark 5: According to (21) and the properties of $\mathscr{S}_i(t)$, one can obtain that $-L_1(t) < e_1 < H_1(t), -L_i(t) < x_i < H_i(t)$ for $\forall t \in [t_{s,j}^i, t_{e,j}^i]$, $j = 1, \ldots, k^i$, and when $t \in (0, t_{s,1}^i) \cup \ldots (t_{e,j}^i, t_{s,j+1}^i) \ldots \cup (t_{e,k^i}^i, +\infty)$, one has $-L_i(t)/\mathscr{S}_i(t) \to -\infty$ and $H_i(t)/\mathscr{S}_i(t) \to +\infty$, which means $-\infty < x_i < +\infty$. It is important to note that the function $\mathscr{S}_i(t)$ plays the role of "stretching" the original constraint boundary to an infinite boundary when no constraint is needed, so we call $\mathscr{S}_i(t)$ "stretching function." In fact, this article deals with intermittent state constraints in a "continuous" way, which is fundamentally different from the control of switched system.

Remark 6: For T/L-HBLF-based schemes [13], [14], [15], [16], they are essentially transformed into constraints on errors, since the errors involve the virtual control functions, so the FC need to be satisfied (see Remark 4 in [19] for details). From (19), the designed NMF only contain state variables, so the proposed scheme effectively remove the FC. Note that the NMF-based algorithms proposed in [17], [18], [19], and [20] can also remove the FC, but the above schemes are only applicable to continuous state constrained HONSs, while the proposed scheme can effectively deal with the intermittent state constraints. Furthermore, the limitation that tracking error dependent on constraint boundaries in [17], [18], and [19] is also removed in this article (see Remark 8). It is worth noting that the idea of stretch model-based is inspired by [12], which considers only one constraint interval, while k^i constraint intervals are considered in this article. It is obvious that the proposed method has a wider range of application. In addition, this article considers the PPTC of state-constrained HONSs, while the method proposed in [12] is limited to the asymptotic tracking control of second-order strict-feedback systems with output constraints.

Let $\mathscr{H}_i = \hbar_{i1}\hbar_{i2}$, from (19), one has

$$\begin{cases} \dot{\chi}_1 = \mu_1\dot{e}_1 + \upsilon_1 \\ \dot{\chi}_i = \mu_i\dot{x}_i + \upsilon_i, i = 2, \ldots, n \end{cases} \tag{22}$$

where $\mu_i = (\mathscr{H}_i + 2m\eta_i^{2m}b_{i1})/\mathscr{H}_i^2, b_{i1} = \mathscr{N}_i/L_i^{2m} + \bar{\mathscr{N}}_i/H_i^{2m}, \upsilon_i = 2m\eta_i^{2m-1}b_{i2}/\mathscr{H}_i^2$ with $i = 1, \ldots, n$, and

$$b_{12} = \left(\frac{e_1\dot{\mathscr{S}}_1L_1 - \eta_1\dot{L}_1}{L_1^{2m+1}}\mathscr{N}_1 + \frac{e_1\dot{\mathscr{S}}_1H_1 - \eta_1\dot{H}_1}{H_1^{2m+1}}\bar{\mathscr{N}}_1\right)e_1$$

$$b_{i2} = \left(\frac{x_i\dot{\mathscr{S}}_iL_i - \eta_i\dot{L}_i}{L_i^{2m+1}}\mathscr{N}_i + \frac{x_i\dot{\mathscr{S}}_iH_i - \eta_i\dot{H}_i}{H_i^{2m+1}}\bar{\mathscr{N}}_i\right)x_i$$

with $\dot{\mathscr{S}}_i(t) = 0$ for $t \in [t_{s,j}^i, t_{e,j}^i]$.

B. Controller Design

Let $z_1 = \chi_1, z_i = \chi_i - \alpha_{i-1}$, where α_{i-1} denotes the virtual control function with $i = 2, \ldots, n$. From (22), one has

$$\begin{cases} \dot{z}_1 = \mu_1\left(\bar{f}_1(\bar{x}_1, y_d) - \dot{y}_d\right) + G_1\chi_2^{p_1} \\ \dot{z}_i = \mu_i\left(\bar{f}_i(\bar{x}_i, y_d) - \frac{\dot{\alpha}_{i-1}}{\mu_i}\right) + G_i\chi_{i+1}^{p_i} \\ \dot{z}_n = \mu_n\left(\bar{f}_n(\bar{x}_n, y_d) - \frac{\dot{\alpha}_{n-1}}{\mu_n}\right) + G_nu^{p_n} \end{cases} \tag{23}$$

where $i = 2, \ldots, n-1, \bar{f}_i(\bar{x}_i, y_d) = f_i(\bar{x}_i) + \upsilon_i/\mu_i, i = 1, \ldots, n$, $G_i = \mu_i g_i(\bar{x}_i)\mathscr{H}_{i+1}^{p_i}, i = 1, \ldots, n-1$, $G_n = \mu_n g_n(\bar{x}_n)$.

Let $\tilde{\Theta}_i = \Theta_i - \hat{\Theta}_i$, $\hat{\Theta}_i$ denotes the estimation of Θ_i, $\Theta_i = \|\Upsilon_i\|^2$, $i = 1, \ldots, n$. Design α_i and $\dot{\hat{\Theta}}_i$ as

$$\alpha_i \triangleq -\Lambda_i z_i \tag{24}$$

$$\Lambda_i = \left[\frac{1}{\underline{G}_i}\left(\frac{\sigma_i}{P_i}\bar{\kappa}_i + \phi_i\right)\right]^{\frac{1}{p_i}} \tag{25}$$

$$\dot{\hat{\Theta}}_i = \frac{r_i}{4a_i}|z_i|^{P_i-1}\|\Pi_i(\mathbb{Z}_i)\|^2 - \bar{\kappa}_i\hat{\Theta}_i \tag{26}$$

where $\sigma_i = ((p_i - 1)/P_i\nu_i)^{(p_i-1)/P_i}(P_i/(p+1))^{(p+1)/P_i}$, $P_i = p - p_i + 2$, $p = \max_{1\le i\le n}\{p_i\}$, $\bar{\kappa}_i = c_i + \dot{\kappa}(t)/\kappa(t)$, ν_i, c_i, a_i, r_i denote positive constants, $i = 1, \ldots, n$. $\underline{G}_i = \mu_i \underline{g}\mathscr{H}_{i+1}^{p_i}$ with $i = 1, \ldots, n-1$, $\underline{G}_n = \mu_n\underline{g}$, $\alpha_n = u$, ϕ_i will be shown later.

Remark 7: It can be concluded from (19) that the NMF (19) has an inverse function, in other words, x_i can be represented by χ_i. Due to the use of FLSs, it is not necessary to know their specific expressions in this article, and only take the variables included in the nonlinear function as input.

The specific control design process is given below.

Step 1: Select the 1th LF V_1 as

$$V_1 = \frac{1}{P_1}z_1^{P_1} + \frac{1}{2r_1}\tilde{\Theta}_1^2. \tag{27}$$

From (23) and (27), we have

$$\begin{aligned} \dot{V}_1 &= \mu_1 z_1^{P_1-1}\left(\bar{f}_1(\bar{x}_1, y_d) - \dot{y}_d\right) + G_1 z_1^{P_1-1}\chi_2^{p_1} - \frac{\tilde{\Theta}_1\dot{\hat{\Theta}}_1}{r_1} \\ &= z_1^{P_1-1}\mathscr{F}_1(\mathbb{Z}_1) + G_1 z_1^{P_1-1}\left(\chi_2^{p_1} - \alpha_1^{p_1}\right) - \frac{\tilde{\Theta}_1\dot{\hat{\Theta}}_1}{r_1} \\ &\quad - \frac{P_1 - 1}{P_1}z_1^{P_1} - G_1\psi_1 z_1^{p+1} + G_1 z_1^{P_1-1}\alpha_1^{p_1} \end{aligned} \tag{28}$$

where $\mathscr{F}_1(\mathbb{Z}_1) = (P_1 - 1)z_1/P_1 + \mu_1(\bar{f}_1(\bar{x}_1, y_d) - \dot{y}_d) + G_1\psi_1 z_1^{p_1}$, $\mathbb{Z}_1 = [\bar{x}_1, y_d, \dot{y}_d]^T$, ψ_1 will be shown later.

This article adopts the FLS to approximate $\mathscr{F}_i(\mathbb{Z}_i)$, i.e., $\mathscr{F}_i(\mathbb{Z}_i) = \Delta_i(\mathbb{Z}_i) + \Upsilon_i^T\Pi_i(\mathbb{Z}_i)$, where $|\Delta_i(\mathbb{Z}_i)| \leq \Delta_i$, and $\Delta_i \in R^+$.

Based on Lemmas 3-4, one has

$$\begin{aligned} z_1^{P_1-1}\mathscr{F}_1(\mathbb{Z}_1) &= z_1^{P_1-1}\left(\Upsilon_1^T\Pi_1(\mathbb{Z}_1) + \Delta_1(\mathbb{Z}_1)\right) \\ &\leq \frac{|z_1|^{P_1-1}\tilde{\Theta}_1\|\Pi_1(\mathbb{Z}_1)\|^2}{4a_1} + \frac{\Delta_1^{P_1}}{P_1} \\ &\quad + \frac{P_1-1}{P_1}z_1^{P_1} + z_1^{p+1}\phi_1 + \delta_1 \end{aligned} \tag{29}$$

where a_1 and δ_1 denote positive constants, and

$$\Psi_1 = \frac{\sqrt{1+\hat{\Theta}_1^2}\|\Pi_1(\mathbb{Z}_1)\|^2}{4a_1} + a_1,$$

$$\phi_1 = \left[\frac{(P_1-1)\Psi_1}{p+1}\right]^{\frac{p+1}{P_1-1}}\left[\frac{p_1}{(P_1-1)\delta_1}\right]^{\frac{p_1}{P_1-1}}.$$

From (24) and (25), we have

$$G_1 z_1^{P_1-1}\alpha_1^{p_1} \leq -\frac{\sigma_1}{P_1}\bar{\kappa}_1 z_1^{p+1} - \phi_1 z_1^{p+1}. \tag{30}$$

From Lemma 3, we can obtain

$$G_1 z_1^{P_1-1}\left(\chi_2^{p_1} - \alpha_1^{p_1}\right) \leq \frac{p_1+1}{p+1}G_1 z_2^{p+1} + G_1\psi_1 z_1^{p+1} \tag{31}$$

where

$$\Xi_1 = p_1\left(2^{p_1-2}+2\right)$$

$$\psi_1 = \frac{(P_1-1)\Xi_1^{\frac{p+1}{P_1-1}} + p\left(\Xi_1|\Lambda_1|^{p_1-1}\right)^{\frac{p+1}{p}}}{p+1}.$$

Substituting (26) and (29)–(31) to (28), we have

$$\dot{V}_1 \leq -\frac{\sigma_1\bar{\kappa}_1}{P_1}z_1^{p+1} + \frac{\bar{\kappa}_1}{r_1}\tilde{\Theta}_1\hat{\Theta}_1 + \frac{p_1+1}{p+1}G_1 z_2^{p+1} + \varrho_1 \tag{32}$$

where $\varrho_1 = \delta_1 + \Delta_1^{P_1}/P_1$.

Step i ($i = 2, \ldots, n-1$): Select the ith LF V_i as

$$V_i = V_{i-1} + \frac{1}{P_i}z_i^{P_i} + \frac{1}{2r_i}\tilde{\Theta}_i^2. \tag{33}$$

Then, one can obtain

$$\begin{aligned} \dot{V}_i \leq &-\sum_{j=1}^{i-1}\left(\frac{\sigma_j\bar{\kappa}_j}{P_j}z_j^{p+1} - \frac{\bar{\kappa}_j}{r_j}\tilde{\Theta}_j\hat{\Theta}_j - \varrho_j\right) - \frac{\tilde{\Theta}_i\dot{\hat{\Theta}}_i}{r_i} \\ &+ z_i^{P_i-1}\mathscr{F}_i(\mathbb{Z}_i) + G_i z_i^{P_i-1}\left(\chi_{i+1}^{p_i} - \alpha_i^{p_i}\right) \\ &+ G_i z_i^{P_i-1}\alpha_i^{p_i} - \frac{P_i-1}{P_i}z_i^{P_i} - G_i\psi_i z_i^{p+1} \end{aligned} \tag{34}$$

where $\mathscr{F}_i(\mathbb{Z}_i) = \mu_i\bar{f}_i(\bar{x}_i, y_d) - \dot{\alpha}_{i-1} + (P_i-1)z_i/P_i + G_i\psi_i z_i^{p_i} + [(p_{i-1}+1)G_{i-1}z_i^{p_i}]/(p+1)$, $\varrho_j = \delta_j + \Delta_j^{P_j}/P_j$. ψ_i will be shown later.

On the basis of Lemmas 3-4, one can obtain

$$\begin{aligned} z_i^{P_i-1}\mathscr{F}_i(\mathbb{Z}_i) \leq &\frac{|z_i|^{P_i-1}\tilde{\Theta}_i\|\Pi_i(\mathcal{Z}_i)\|^2}{4a_i} + \frac{\Delta_i^{P_i}}{P_i} \\ &+ \frac{P_i-1}{P_i}z_i^{P_i} + \phi_i z_i^{p+1} + \delta_i \end{aligned} \tag{35}$$

where a_i and δ_i denote positive constants, and

$$\Psi_i = \frac{\sqrt{1+\hat{\Theta}_i^2}\|\Pi_i(\mathbb{Z}_i)\|^2}{4a_i} + a_i$$

$$\phi_i = \left[\frac{(P_i-1)\Psi_i}{p+1}\right]^{\frac{p+1}{P_i-1}}\left[\frac{p_i}{(P_i-1)\delta_i}\right]^{\frac{p_i}{P_i-1}}.$$

Based on Lemma 3, we have

$$G_i z_i^{P_i-1}\left(\chi_{i+1}^{p_i} - \alpha_i^{p_i}\right) \leq \frac{p_i+1}{p+1}G_i z_{i+1}^{p+1} + G_i\psi_i z_i^{p+1} \tag{36}$$

where

$$\Xi_i = p_i\left(2+2^{p_i-2}\right)$$

$$\psi_i = \frac{(P_i-1)\Xi_i^{\frac{p+1}{P_i-1}} + p\left(\Xi_i|\Lambda_i|^{p_i-1}\right)^{\frac{p+1}{p}}}{p+1}.$$

Substituting (24)–(26) and (35)–(36) into (34), one can obtain

$$\begin{aligned} \dot{V}_i \leq &-\sum_{j=1}^{i}\frac{\sigma_j\bar{\kappa}_j}{P_j}z_j^{p+1} + \sum_{j=1}^{i}\frac{\bar{\kappa}_j}{r_j}\tilde{\Theta}_j\hat{\Theta}_j \\ &+ \sum_{j=1}^{i}\varrho_j + \frac{p_i+1}{p+1}G_i z_{i+1}^{p+1}. \end{aligned} \tag{37}$$

Step n: Select the nth LFc V_n as

$$V_n = V_{n-1} + \frac{1}{P_n}z_n^{P_n} + \frac{1}{2r_n}\tilde{\Theta}_n^2. \tag{38}$$

From (38), we have

$$\begin{aligned} \dot{V}_n \leq &-\sum_{j=1}^{n-1}\left(\frac{\sigma_j\bar{\kappa}_j}{P_j}z_j^{p+1} - \frac{\bar{\kappa}_j}{r_j}\tilde{\Theta}_j\hat{\Theta}_j - \varrho_j\right) - \frac{\tilde{\Theta}_n\dot{\hat{\Theta}}_n}{r_n} \\ &+ z_n^{P_n-1}\mathscr{F}_n(\mathbb{Z}_n) + G_n z_n^{P_n-1}u^{p_n} - \frac{P_n-1}{P_n}z_n^{P_n} \end{aligned} \tag{39}$$

where $\mathscr{F}_n(\mathbb{Z}_n) = \mu_n\bar{f}_n(\bar{x}_n, y_d) - \dot{\alpha}_{n-1} + (P_n-1)z_n/P_n + [(p_{n-1}+1)G_{n-1}z_n^{p_n}]/(p+1)$.

Similar to (29) and (35), one has

$$\begin{aligned} z_n^{P_n-1}\mathscr{F}_n(\mathbb{Z}_n) \leq &\frac{|z_n|^{P_n-1}\tilde{\Theta}_n\|\Pi_n(\mathbb{Z}_n)\|^2}{4a_n} + \frac{\Delta_n^{P_n}}{P_n} \\ &+ \frac{P_n-1}{P_n}z_n^{P_n} + \phi_n z_n^{p+1} + \delta_n \end{aligned} \tag{40}$$

where a_n and δ_n denote positive constants, and

$$\Psi_n = \frac{\sqrt{1+\hat{\Theta}_n^2}\|\Pi_n(\mathbb{Z}_n)\|^2}{4a_n} + a_n$$

$$\phi_n = \left[\frac{(P_n-1)\Psi_n}{p+1}\right]^{\frac{p+1}{P_n-1}}\left[\frac{p_n}{(P_n-1)\delta_n}\right]^{\frac{p_n}{P_n-1}}.$$

Substituting (24)–(26) and (40) into (39), one has

$$\dot{V}_n \leq -\sum_{j=1}^{n}\frac{\sigma_j\bar{\kappa}_j}{P_j}z_j^{p+1} + \sum_{j=1}^{n}\frac{\bar{\kappa}_j}{r_j}\tilde{\Theta}_j\hat{\Theta}_j + \sum_{j=1}^{n}\varrho_j. \tag{41}$$

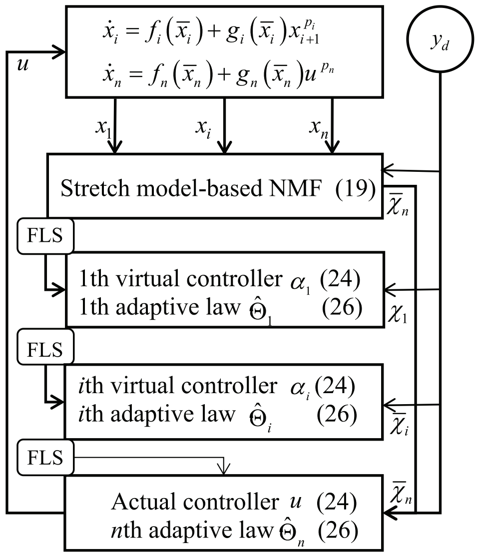

Fig. 2. Block diagram of the proposed algorithm.

It can be obtained from Lemma 4 that $z_i^{P_i} \leq \nu_i + z_i^{p+1}\sigma_i$, then $-z_i^{p+1} \leq (-z_i^{P_i} + \nu_i)/\sigma_i$, $i = 1, \ldots, n$. Then, one has

$$\dot{V}_n \leq -\sum_{j=1}^{n} \frac{\bar{\kappa}_j}{P_j} z_j^{P_j} + \sum_{j=1}^{n} \frac{\bar{\kappa}_j}{r_j} \tilde{\Theta}_j \hat{\Theta}_j + \sum_{j=1}^{n} \left(\varrho_j + \frac{\nu_i}{\sigma_j} \right). \quad (42)$$

Since $\tilde{\Theta}_j \hat{\Theta}_j \leq -\tilde{\Theta}_j^2/2 + \Theta_j^2/2$, then we have

$$\dot{V}_n \leq -\sum_{j=1}^{n} \frac{\bar{\kappa}_j}{P_j} z_j^{P_j} - \sum_{j=1}^{n} \frac{\bar{\kappa}_j \tilde{\Theta}_j^2}{2r_j} + \varrho \quad (43)$$

where $\varrho = \sum_{j=1}^{n} (\varrho_j + \nu_j/\sigma_j) + \sum_{j=1}^{n} (\bar{\kappa}_j \Theta_j^2)/(2r_j)$.

Let $c = \min_{1 \leq i \leq n}\{c_i\}$, based on the expression of $\bar{\kappa}_i$, we can obtain

$$\dot{V}_n \leq -cV_n - \frac{\dot{\kappa}(t)}{\kappa(t)} V_n + \varrho. \quad (44)$$

The block diagram of the proposed algorithm is given in Fig. 2

C. Stability Analysis

The stability analysis is concluded by the following Theorem.

Theorem For HONS (1) with $x(0) \in \mathscr{B}_x$ and Assumptions 1-2, the designed control scheme ensures

$\mathscr{O}_1$) All signals of HONS (1) are semi-globally bounded.

$\mathscr{O}_2$) The intermittent state constraints are not transgressed without involving the FC.

$\mathscr{O}_3$) The system output y tracks the desired signal y_d within a prescribed time.

Proof:

$\mathscr{O}_1$): According to Lemma 1 and (44), it can be known that the designed control algorithm ensures that the closed-loop system is PPTS, and

$$V_n \leq \frac{V_n(0)e^{-t}}{(1+\varepsilon)\kappa(t)} + \frac{\varrho}{c\varepsilon\kappa(t)}. \quad (45)$$

Then, one can know from (45) that

$$V_n \leq \varepsilon V_n(0) + \frac{\varrho}{c} \quad \forall t \geq T. \quad (46)$$

According to the expression of V_n, one know that z_i and $\tilde{\Theta}_i$ are bounded. From (24)–(26), α_i,u and $\hat{\Theta}_i$ are bounded. Since $z_1 = \chi_1, z_i = \chi_i - \alpha_{i-1}$, so χ_i is bounded. From (17)–(19), one has $0 < \hbar_{i1}\hbar_{i2} < 1$ and $e_1 = \chi_1\hbar_{11}\hbar_{12}, x_i = \chi_i\hbar_{i1}\hbar_{i2}$, so the boundedness of x_i can be ensured. To sum up, all the closed-loop signals are semi-globally bounded.

$\mathscr{O}_2$): $x(0) \in \mathscr{B}_x$ means $\eta_i(0) \in (-L_i(0), H_i(0))$, On the basis of the boundedness of χ_i, one can obtain that $\eta_i \in (-L_i, H_i)$. From the expressions of η_i and $\mathscr{S}_i$, one can further obtain that $x \in \mathscr{B}_x$ for $\forall t \in [t_{s,j}^i, t_{e,j}^i]$. If $t \in (0, t_{s,1}^i) \cup \cdots (t_{e,j}^i, t_{s,j+1}^i) \cdots \cup (t_{e,k^i}^i, +\infty)$, one has $-L_i/\mathscr{S}_i \to -\infty$ and $H_i/\mathscr{S}_i \to +\infty$, which means $-\infty < x_i < +\infty$, i.e., the intermittent state constraints are not violated. Furthermore, Remark 6 illustrates that the proposed scheme removes the FC.

$\mathscr{O}_3$): According to (46) and the expression of V_n, one has

$$|z_1| \leq \left[P_1 \left(\varepsilon V_n(0) + \frac{\varrho}{c} \right) \right]^{\frac{1}{P_1}} \quad \forall t \geq T. \quad (47)$$

Since $z_1 = \chi_1 = e_1/(\hbar_{11}\hbar_{12})$ and $0 < \hbar_{11}\hbar_{12} < 1$, then one has $|e_1| \leq |z_1|$, which means that the system output y tracks the desired signal y_d within a prescribed time. ■

Remark 8: In contrast to recent NMF-based approaches [12], [17], [18], [19], the proposed algorithm can not only remove the FC and be effective for intermittent state-constrained HONSs (see Remarks 5-6), but also has the advantage of accurately analyzing the range of tracking error, i.e., $|e_1| \leq |z_1|$. According to the analysis of [12], [17], [18], and [19], $e_1 = z_1\wp$, $\wp = (L_1 + e_1)(H_1 - e_1)$. Apparently, the range of tracking error e_1 relies on the constraint functions and can not be analyzed accurately.

Remark 9: In particular, it is worth noting that the presented algorithm is a unified one that can be applied to HONSs with conventional continuous state constraints/deferred state constraints/ funnel constraints or constraints-free without changing the control structure.

1) Select $t_{s,k^i}^i = 0, t_{e,k^i}^i = +\infty$, it can be obtained from (15) that $\mathscr{S}_i \equiv 1$ for $\forall t \in [0, +\infty)$, so the barrier function (17) in this article is equivalent to that in [20], i.e., the proposed method can handle conventional continuous state constraints [20].
2) Select $t_{e,k^i}^i = 0$, it means that the system does not encounter state constraints. In this case, it can be known from Remark 5 that $-L_i/\mathscr{S}_i \to -\infty, H_i/\mathscr{S}_i \to +\infty$, so the proposed method also applies to unconstrained HONSs.
3) Select $t_{s,1}^i = t_0, t_{e,1}^i = +\infty$ (t_0 denotes a positive design constant), which means that there is no constraint when $t \in [0, t_0)$, when $t \in [t_0, +\infty)$ system encounters constraints. This situation is actually similar to the deferred state constraints proposed in [50].
4) Select $t_{s,k^1}^1 = 0, t_{e,k^1}^1 = +\infty, t_{e,k^i}^i = 0 (i \geq 2)$, and the constraint boundaries $-L_1$ and H_1 are taken as the performance-constrained functions, the proposed

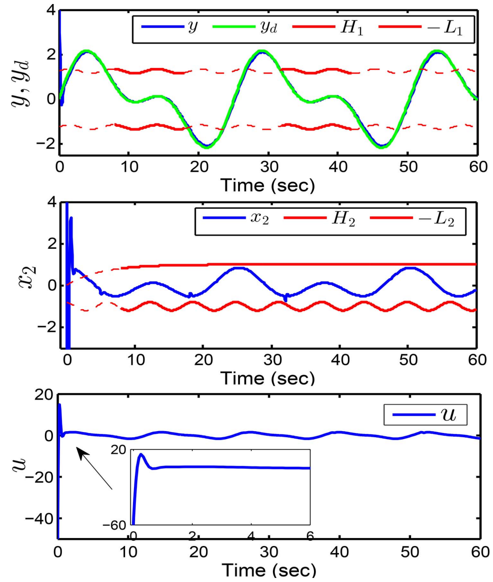

Fig. 3. Simulation results under intermittent state constraints.

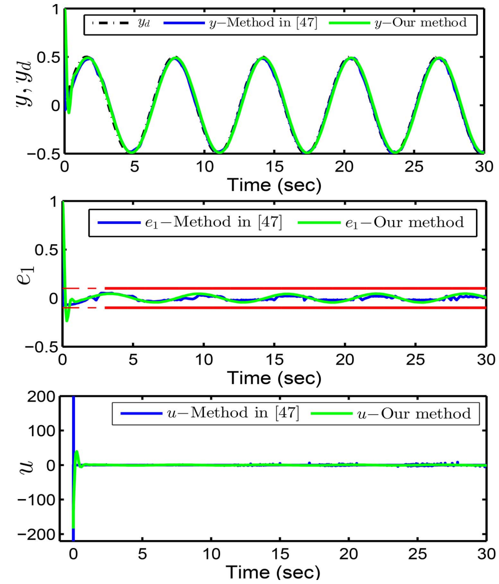

Fig. 4. Simulation results compared with the method in [47].

technique is a solution to prescribed performance control (or funnel control) [51], [52]. Furthermore, if select $t^1_{s,k^1} = t_0 > 0, t^1_{e,k^1} = +\infty, t^i_{e,k^i} = 0 (i \geq 2)$, $t_0 > 0$ represents a design constant, the proposed method can guarantee that the tracking error with large initial values (even arbitrary bounded initial values) can enter the constraint boundaries within t_0, and then satisfies the funnel constraints.

Remark 10: It should be noted that in order to make the algorithm more flexible, the proposed algorithm involves some design parameters. According to the bounded analysis of the system, the tracking performance can be improved by appropriately increasing r_i and ε, or decreasing ν_i. In practice, it may be necessary to take into account a variety of performance, such as control energy, tracking performance, and so on, so the parameters need to be adjusted according to the actual needs.

IV. Simulation

Example 1: Given a HONS as

$$\begin{cases} \dot{x}_1 = f_1(\bar{x}_1) + g_1(\bar{x}_1)x_2^{p_1} \\ \dot{x}_2 = f_2(\bar{x}_2) + g_2(\bar{x}_2)u^{p_2} \\ y = x_1 \end{cases} \tag{48}$$

where $f_1(\bar{x}_1) = x_1 e^{-0.5x_1}, f_2(\bar{x}_2) = -3x_1 - 0.5x_2, g_1(\bar{x}_1) = g_2(\bar{x}_2) = 1$. Let $y_d = \sin(0.5t) + 1.5\sin(0.25t)$, $p_1 = 1, p_2 = 3, c_i = 25, a_i = 1, r_i = 50$ with $i = 1, 2$, $\epsilon = 0.0001$, $T = 4, L_1 = 1.25 - 0.1\sin t$, $H_1 = 1.25 + 0.1\sin t$, $L_2 = 1 + 0.2\sin(5 + t)$, $H_2 = 1 - 2^{-0.3t}$, $t^1_{s,1} = 8, t^1_{e,1} = 18, t^1_{s,2} = 32, t^1_{e,2} = 42, t^2_{s,1} = 8, t^2_{e,1} = +\infty$, $\hat{\Theta}_i(0) = 0.1$ with $i = 1, 2, \bar{x}_2(0) = [5, 4.2]^T$. Fig. 3 gives the curves of y_d, y, x_2 and its constraint boundaries, and the curve of u, respectively. It can be known from Fig. 3 that the proposed algorithm can ensure that y tracks y_d within the prescribed time T, and the intermittent state constraints are not transgressed.

In order to further demonstrate the superiority of the proposed PPTC algorithm, we compare the proposed approach with that of [47]. For system (48), let $p_1 = p_2 = 1$, $t^1_{s,1} = 1$, $t^1_{e,1} = +\infty, t^2_{s,k^2} = 0, t^2_{e,k^2} = +\infty, y_d = 0.5\sin(t), L_1 = H_1 = 0.1, \bar{x}_2 = [1, 1.2]^T$. It can be known from Fig. 4 that the proposed PPTC approach can achieve the same practical prescribed-time tracking performance as in [47], while the initial control input of the proposed algorithm is much smaller than that in [47].

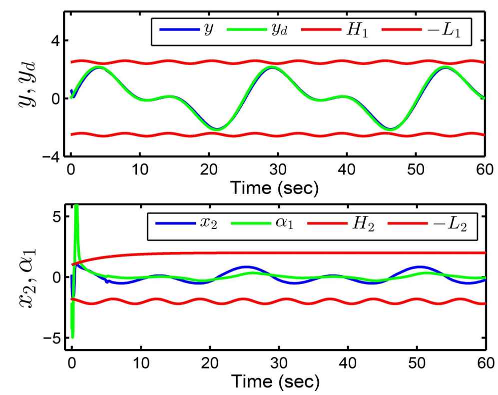

Fig. 5. Simulation results under full-state constraints.

The simulation results under full-state constraints are shown in Fig. 5, where $L_1 = 2.5 - 0.1\sin t$, $H_1 = 2.5 + 0.1\sin t$, $L_2 = 1 + 0.2\sin(5 + t)$, $H_2 = 1 - 2^{-0.3t}$, $t^i_{s,k^i} = 0, t^i_{e,k^i} = +\infty$. It can be seen from Fig. 5 that y tracks y_d within the prescribed time, and the full-state constraints are not transgressed. Meanwhile, the virtual control function α_1 is not within the constraint boundaries. Note that the existing T/L-HBLF-based methods [13], [14], [15], [16] require the virtual control function α_1 to be within the constraint boundaries (i.e., the FC), so the proposed algorithm deals with the state constraints without involving the FC. Indeed, the proposed method under full state constraints degenerates to the results in [20]. In this case, the advantage of the proposed scheme is that the settling time can be arbitrarily set, while it depends on the control parameters in [20]. Furthermore, the method proposed in [20] requires that the initial states of the system must be within the constraint boundaries, while the proposed method is applicable to any

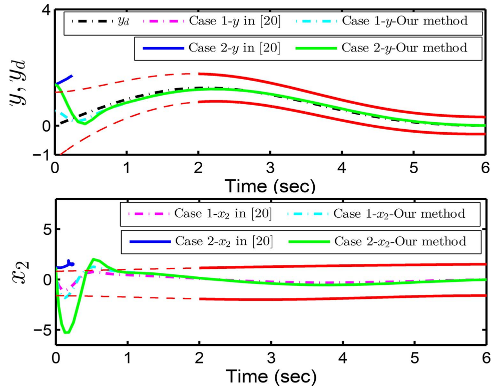

Fig. 6. Simulation results compared with the method in [20].

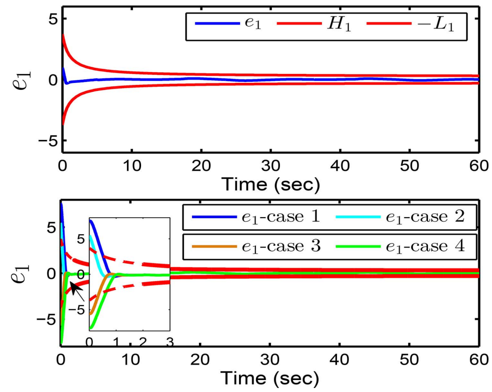

Fig. 7. Simulation results under funnel constraints.

bounded initial states. To verify this, select the following two initial states, case 1: $\bar{x}_2(0) = [0.5, 0.4]^T \in (-L_i(0), H_i(0))$ and case 2: $\bar{x}_2(0) = [1.4, 1.2]^T \notin (-L_i(0), H_i(0))$. Fig. 6 shows the comparison results, it can be obtained from Fig. 6 that the proposed method is applicable to cases 1 and 2, while the method proposed in [20] is only applicable to case 1.

Let $t^1_{s,k^1} = 0$, $t^1_{e,k^1} = +\infty$, $t^2_{e,k^2} = 0$,$L_1 = 0.15+3.5/(t+1)$, $H_1 = 0.15+3.5/(t+1)$, $L_2 = 1+0.2\sin(5+t)$, $H_2 = 1-2^{-0.3t}$, the simulation result is shown in the upper subgraph of Fig. 7. It is worth noting that the conventional prescribed performance control (or funnel control) requires that the initial tracking error must be within the constraint range, i.e., $-L_1(0) < e_1(0) < H_1(0)$. While the proposed method can ensure that the tracking error with any bounded initial values can enter the preset boundaries within a preset time. To verify this, let $t^1_{s,k^1} = 2$, $t^1_{e,k^1} = +\infty$, $t^2_{e,k^2} = 0$. We choose the following four different initial states: case 1: $\bar{x}_2(0) = [7.5, 5.2]^T$; case 2: $\bar{x}_2(0) = [5.5, 5.2]^T$; case 3: $\bar{x}_2(0) = [-5.5, -5.2]^T$; and case 4: $\bar{x}_2(0) = [-7.5, -5.2]^T$. The subgraph in Fig. 8 shows the simulation result under four initial conditions, which means that the proposed method can guarantee that the tracking error with large initial values (even arbitrary bounded initial values) can enter the constraint boundaries within a preset time, and then satisfies the funnel constraints.

Remark 11: It is noted that although the proposed method removes singularity of existing STF-based PTC methods [35], [36], [37], [38], [39], [40], [41], [44], [45], the control input

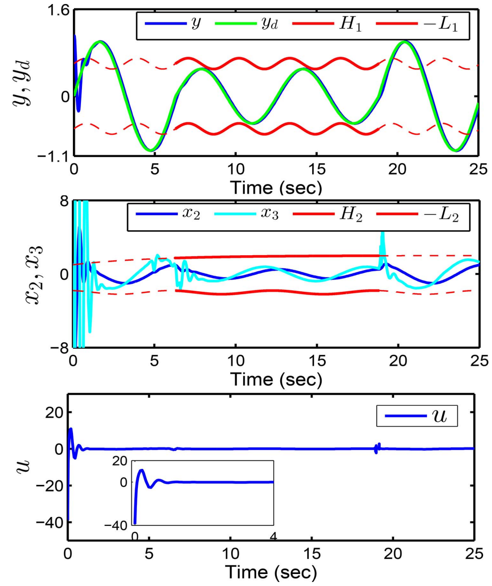

Fig. 8. Simulation results under intermittent state constraints.

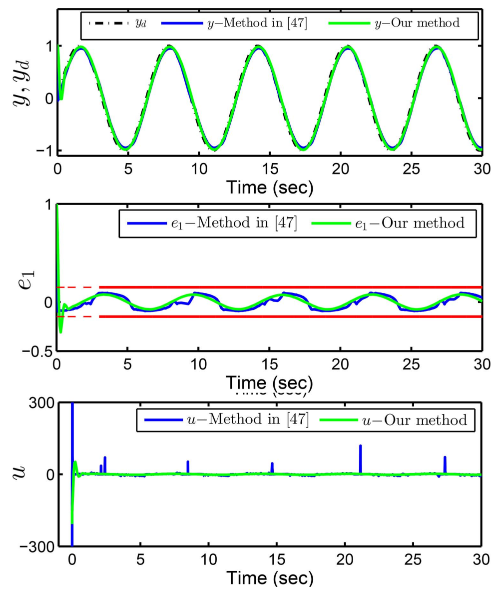

Fig. 9. Simulation results compared with the method in [47].

still has a small fluctuation at the prescribed-time point (see Figs. 3 and 4). The main reason is that the designed STF should ensure the prescribed-time stable of the system, and the STF will have a large change at the prescribed-time point, which is inevitable. In fact, in the existing PTC algorithms, the STF is discontinuous at the prescribed-time point, so it will produce singularity, but the designed STF is continuously derivable, so the singularity is effectively removed.

Example 2: Consider a simple direct-driven single-link manipulator model [47] as follows:

$$\begin{cases} \dot{x}_1 = x_2 \\ \dot{x}_2 = \frac{E}{\mathcal{P}}\sin x_1 - \frac{S}{\mathcal{P}}x_2 + \frac{0.1}{\mathcal{P}}x_1\sin x_2 + \frac{1}{\mathcal{P}}x_3 \\ \dot{x}_3 = \frac{K_B}{\mathcal{L}}x_2 - \frac{R}{\mathcal{L}}x_3 + \frac{1}{\mathcal{L}}\left(1+x_1^2\right)u \\ y = x_1 \end{cases} \tag{49}$$

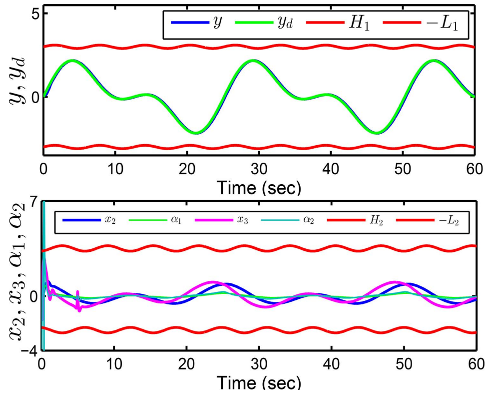

Fig. 10. Simulation results under full-state constraints.

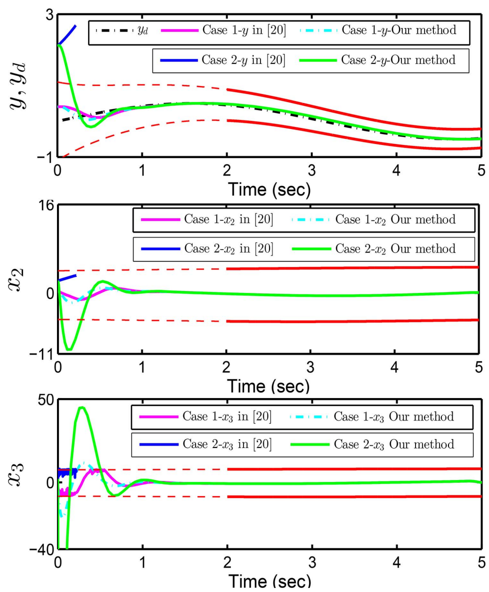

Fig. 11. Simulation results compared with the method in [20].

where x_1, x_2 and x_3 denote the angular position, velocity and the armature current, respectively. u represents an voltage. Choose $E = 10, \mathcal{P} = 1 = S = 1, \mathcal{L} = 0.05, K_B = R = 0.5$. Let $y_d = 0.5 \sin t$ for $t \in (2\pi, 6\pi)$, and $y_d = \sin t$ for $t \in [0, 2\pi] \cup [6\pi, 25]$,$c_i = 25, a_i = 1, r_i = 50$ with $i = 1, 2, 3$, $\epsilon = 0.0001$, $T = 3$,$t^1_{s,1} = t^2_{s,1} = t^3_{s,1} = 2\pi, t^1_{e,1} = t^2_{e,1} = t^3_{e,1} = 6\pi$,$\hat{\Theta}_i(0) = 0.1$ with $i = 1, 2, 3$,$\bar{x}_3(0) = [1.1, 1.2, 1.1]^T$. The results are shown in Fig. 8. It can be known from Fig. 8 that y can track y_d within a prescribed time, and the intermittent state constraints are not transgressed.

The simulation results compared with the method in [47] are shown in Fig. 9, which means that the proposed PPTC approach can achieve the same control performance as the method proposed in [47] with smaller control energy consumption. The simulation results under full-state constraints and funnel constraints are give in Figs. 10 and 12, which means that the proposed algorithm can deal with the conventional full-state constraints and funnel constraints. The simulation results compared with the method in [20] are shown in Fig. 11, which shows that the proposed method is applicable to any bounded initial state, while the method in [20] requires that the initial state must be within the constraint boundaries.

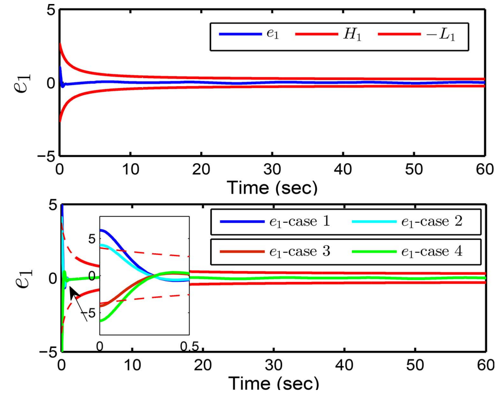

Fig. 12. Simulation results under funnel constraints.

V. Conclusion

In this article, a more relaxed sufficient condition for PPTS is given, based on which a novel PPTC algorithm for intermittent state constrained HONSs is designed. The proposed algorithm can preset the settling time, which does not depend on the initial state of the system, and the limitations of singularity and excessive initial control input in existing methods are overcome. Moreover, by designing a novel stretch model-based NMF, the intermittent state constraints are handled under removal FC. The results show that the proposed algorithm is a unified scheme, which is also applicable to HONSs with conventional continuous state constraints/deferred state constraints/funnel constraints or constraints-free without changing the control structure. In the future, we will focus on the PPTC for intermittent state-constrained stochastic HONSs. In addition, the proposed algorithm is designed based on Assumptions 1-2, so removing these assumptions is also the direction of future efforts.

References

[1] F. Blanchini, "Set invariance in control," *Automatica*, vol. 35, no. 11, pp. 1747–1767, 1999.

[2] A. Bemporad, "Reference governor for constrained nonlinear systems," *IEEE Trans. Autom. Control*, vol. 43, no. 3, pp.415-419, Mar. 1998.

[3] D. Q. Mayne, J. B. Rawlings, C. V. Rao, and P. O. M. Scokaert, "Constrained model predictive control: Stability and optimality," *Automatica*, vol. 36, no. 6, pp. 789-814, Jun. 2000.

[4] K. P. Tee, S. S. Ge, and E. H. Tay, "Barrier Lyapunov functions for the control of output-constrained nonlinear systems," *Automatica*, vol. 45, no. 4, pp. 918–927, Apr. 2009.

[5] K. P. Tee, B. B. Ren, and S. S. Ge, "Control of nonlinear systems with time-varying output constraints," *Automatica*, vol. 47, no. 11, pp. 2511–2516, 2011.

[6] Y. J. Liu and S. C. Tong, "Barrier Lyapunov functions for Nussbaum gain adaptive control of full state constrained nonlinear systems," *Automatica*, vol. 76, no. 2, pp. 143–152, Feb. 2017.

[7] W. W. Sun, Y. Wu, and X. Y. Lv, "Adaptive neural network control for full-state constrained robotic manipulator with actuator saturation and time-varying delays," *IEEE Trans. Neural Netw. Learn. Syst.*, vol. 33, no. 8, pp. 3331–3342, Jan. 2022.

[8] K. Zhao and Y. Song, "Removing the feasibility conditions imposed on tracking control designs for state-constrained strict-feedback systems," *IEEE Trans. Autom. Control*, vol. 64, no. 3, pp. 1265–1272, Mar. 2019.

[9] Y. Cao, C. Wen, and Y. Song, "A unified event-triggered control approach for uncertain pure-feedback systems with or without state constraints," *IEEE Trans. Cybern.*, vol. 51, no. 3, pp. 1262–1271, Mar. 2021.

[10] Y. Yao, J. Tan, J. Wu, and X. Zhang, "Event-triggered fixed-time adaptive fuzzy control for state-constrained stochastic nonlinear systems without feasibility conditions," *Nonlin. Dyn.*, vol. 105, pp. 403–416, Jun. 2021.

[11] Y. Yao, J. Tan, J. Wu, and X. Zhang, "Decentralized fixed-time control for state-constrained stochastic systems via nonlinear state-dependent function approach," *Int. J. Robust Nonlin. Control.*, vol. 32, no. 8, pp. 4923–4945, May 2022.

[12] L. Kong, W. He, Z. Liu, X. Yu, and C. Silvestre, "Adaptive tracking control with global performance for output-constrained MIMO nonlinear systems," *IEEE Trans. Autom. Control*, vol. 68, no. 6, pp. 3760–3767, Jun. 2023, doi: 10.1109/TAC.2022.3201258.

[13] N. Wang, F. Tao, Z. Fu, and S. Song, "Adaptive fuzzy control for a class of stochastic strict feedback high-order nonlinear systems with full-state constraints," *IEEE Trans. Syst., Man, Cybern. Syst.*, vol. 52, no. 1, pp. 205–213, Jan. 2022.

[14] Y. Wu and X.-J. Xie, "Adaptive fuzzy control for high-order nonlinear time-delay systems with full-state constraints and input saturation," *IEEE Trans. Fuzzy Syst.*, vol. 28, no. 8, pp. 1652–1663, Aug. 2020.

[15] W. Sun, S.-F. Su, Y. Wu, J. Xia, and V.-T. Nguyen, "Adaptive fuzzy control with high-order barrier Lyapunov functions for high-order uncertain nonlinear systems with full-state constraints," *IEEE Trans. Cybern.*, vol. 50, no. 8, pp. 3424–3432, Aug. 2020.

[16] W. Sun, S.-F. Su, G. Dong, and W. Bai, "Reduced adaptive fuzzy tracking control for high-order stochastic nonstrict feedback nonlinear system with full-state constraints," *IEEE Trans. Syst., Man, Cybern., Syst.*, vol. 51, no. 3, pp. 1496–1506, Mar. 2021.

[17] Y. Wu, X.-J. Xie, and Z.-G. Hou, "Adaptive fuzzy asymptotic tracking control of state-constrained high-order nonlinear time-delay systems and its applications," *IEEE Trans. Cybern.*, vol. 52, no. 3, pp. 1671–1680, Mar. 2022.

[18] X.-J. Xie, Y. Wu, and Z.-G. Hou, "Further results on adaptive practical tracking for high-order nonlinear systems with full-state constraints," *IEEE Trans. Cybern.*, vol. 52, no. 10, pp. 9978–9985, Oct. 2022.

[19] Y. Yao, Y. Kang, Y. Zhao, P. Li, and J. Tan, "Unified fuzzy control of high-order nonlinear systems with multitype state constraints," *IEEE Trans. Cybern.*, early access, Apr. 13, 2023, doi: 10.1109/TCYB.2023.3263352.

[20] Y. Yao, J. Tan, J. Wu, and X. Zhang, "A unified fuzzy control approach for stochastic high-order nonlinear systems with or without state constraints," *TEEE Trans Fuzzy Syst.*, vol. 30, no. 10, pp. 4530-4540, Oct. 2022.

[21] C.-C. Chen and Z.-Y. Sun, "A unified approach to finite-time stabilization of high-order nonlinear systems with an asymmetric output constraint," *Automatica*, vol. 111, Jan. 2020, Art. no. 108581.

[22] Z.-Y. Sun, C. Zhou, C. Wen, and C.-C. Chen, "Adaptive event-triggered fast finite-time stabilization of high-order uncertain nonlinear systems and its application in maglev systems," *IEEE Trans. Cybern.*, early access, Nov. 29, 2022, doi: 10.1109/TCYB.2022.3220742.

[23] H. Min, S. Xu, and Z. Zhang, "Adaptive finite-time stabilization of stochastic nonlinear systems subject to full-state constraints and input saturation," *IEEE Trans. Autom. Control.*, vol. 66, no. 3, pp. 1306–1313, Mar. 2021.

[24] X. Min, S. Baldi, and W. Yu, "Finite-time distributed control of nonlinear multiagent systems via funnel technique," *IEEE Trans. Syst., Man, Cybern., Syst.*,vol. 53, no. 2, pp. 1256–1267, Feb. 2023.

[25] X. Bu, B. Jiang, and H. Lei, "Performance guaranteed finite-time non-affine control of waverider vehicles without function-approximation," *IEEE Trans. Intel. Transp. Syst.*, vol. 24, no. 3, pp. 3252–3262, Mar. 2023.

[26] X. Bu, M. Lv, H. Lei, and J. Cao, "Fuzzy neural pseudo control with prescribed performance for waverider vehicles: A fragility-avoidance approach," *IEEE Trans. Cybern.*, vol. 53, no. 8, pp. 4986–4999, Aug. 2023.

[27] X. Bu, C. Hua, M. Lv, and Z. Wu, "Flight control of waverider vehicles with fragility-avoidance prescribed performance," *IEEE Trans. Aerosp. Electron. Syst.*, vol. 59, no. 5, pp. 5248–5261, Oct. 2023, doi: 10.1109/TAES.2023.3251314.

[28] Y. Yao, J. Tan, J. Wu, and X. Zhang, "Event-triggered finite-time adaptive fuzzy tracking control for stochastic nontriangular structure nonlinear systems," *Int. J. Fuzzy Syst.*, vol. 23, no. 7, pp. 2157–2169, Mar. 2021.

[29] Y. Yao, J. Tan, J. Wu, and X. Zhang, "Event-triggered fixed-time adaptive neural dynamic surface control for stochastic non-triangular structure nonlinear systems," *Inf. Sci.*, vol. 569, pp. 527–543, Aug. 2021.

[30] Y. Yao, J. Tan, J. Wu, X. Zhang, and L. He, "Prescribed tracking error fixed-time control of stochastic nonlinear systems," *Chaos Solitons Fractals*, vol. 160, Jul. 2022, Art. no. 1112288.

[31] J. Ma, H. Wang and J. Qiao, "Adaptive neural fixed-time tracking control for high-order nonlinear systems," *IEEE Trans. Neural Netw. Learn. Syst.*, vol. 35, no. 1, pp. 708–717, Jan. 2024, doi: 10.1109/TNNLS.2022.3176625.

[32] H. Wang, J. Ma, X. Zhao, B. Niu, M. Chen, and W. Wang, "Adaptive fuzzy fixed-time control for high-order nonlinear systems with sensor and actuator faults," *IEEE Trans. Fuzzy Syst.*, vol. 31, no. 8, pp. 2658–2668, Aug. 2023, doi: 10.1109/TFUZZ.2023.3235395.

[33] T. Jia, Y. Pan, H. Liang, and H.-K. Lam, "Event-based adaptive fixed-time fuzzy control for active vehicle suspension systems with time-varying displacement constraint," *IEEE Trans. Fuzzy Syst.*, vol. 30, no. 8, pp. 2813–2821, Aug. 2022.

[34] J. D. Snchez-Torres, E. N. Sanchez, and A. G. Loukianov, "Predefined-time stability of dynamical systems with sliding modes," in *Proc. Amer. Control Conf. (ACC)*, 2015, pp. 5842–5846.

[35] Y. Song, Y. Wang, J. Holloway, and M. Krstic, "Time-varying feedback for regulation of normal-form nonlinear systems in prescribed finite time," *Automatica*, vol. 83, pp. 243–252, Sep. 2017.

[36] C. Hua, P. Ning, and K. Li, "Adaptive prescribed-time control for a class of uncertain nonlinear systems," *IEEE Trans. Autom. Control*, vol. 61, no. 17, pp. 6159–6166, Nov. 2021.

[37] F. Gao, Y. Wu, and Z. Zhang, "Global fixed-time stabilization of switched nonlinear systems: A time-varying scaling transformation approach," *IEEE Trans. Circuits Syst. II, Exp. Briefs*, vol. 66, no. 11, pp. 1890–1894, Nov. 2019.

[38] A. K. Pal, S. Kamal, X. Yu, S. K. Nagar, and X. Xiong, "Free-will arbitrary time consensus for multiagent systems," *IEEE Trans. Cybern.*, vol. 52, no. 6, pp. 4636–4646, Jun. 2022.

[39] W. Li and M. Krstic, "Stochastic nonlinear prescribed-time stabilization and inverse optimality," *IEEE Trans. Autom. Control*, vol. 67, no. 3, pp. 1179–1193, Mar. 2022.

[40] W. Li and M. Krstic, "Prescribed-time output-feedback control of stochastic nonlinear systems," *IEEE Trans. Autom. Control*, vol. 68, no. 3, pp. 1431–1446, Mar. 2023.

[41] Z. Sheng, Q. Ma, and S. Xu, "Prescribed-time output feedback control for high-order nonlinear systems," *IEEE Trans. Circuits Syst. II, Exp. Briefs*, vol. 70, no. 7, pp. 2460–2464, Jul. 2023, doi: 10.1109/TCSII.2023.3241160.

[42] B. Ning, Q. Han, and Z. Zuo, "Practical fixed-time consensus for integrator-type multi-agent systems: A time base generator approach," *Automatica*, vol. 105, pp. 406–414, Jul. 2019.

[43] C. Guo and J. Hu, "Time base generator-based practical predefined-time stabilization of high-order systems with unknown disturbance," *IEEE Trans. Circuits Syst. II, Exp. Briefs*, vol. 70, no. 7, pp. 2670–2674, Jul. 2023, doi: 10.1109/TCSII.2023.3242856.

[44] Z. Wang, H.-K. Lam, B. Xiao, Z. Chen, B. Liang, and T. Zhang, "Event-triggered prescribed-time fuzzy control for space teleoperation systems subject to multiple constraints and uncertainties," *IEEE Trans. Fuzzy Syst.*, vol. 29, no. 9, pp. 2785–2797, Sep. 2021.

[45] Z. Wang et al., "Adaptive event-triggered control for nonlinear systems with asymmetric state constraints: A prescribed-time approach," *IEEE Trans. Autom. Control*, vol. 68, no. 6, pp. 3625–3632, Jun. 2023, doi: 10.1109/TAC.2022.3194880.

[46] H. Xu, D. Yu, S. Sui, and C. L. P. Chen, "An event-triggered predefined time decentralized output feedback fuzzy adaptive control method for interconnected systems," *IEEE Trans. Fuzzy Syst.*, vol. 31, no. 2, pp. 631–644, Feb. 2023.

[47] Q. Wang, J. Cao, and H. Liu, "Adaptive fuzzy control of nonlinear systems with predefined time and accuracy," *IEEE Trans. Fuzzy Syst.*, vol. 30, no. 12, pp. 5152–5165, Dec. 2022.

[48] A.-M. Zou, Y. Liu, Z.-G. Hou, and Z. Hu, "Practical predefined-time output-feedback consensus tracking control for multiagent systems," *IEEE Trans. Cybern.*, vol. 53, no. 8, pp. 5311–5322, Aug. 2023, doi: 10.1109/TCYB.2022.3207325.

[49] J. Wu, J. Li, G. Zong, and W. Chen, "Global finite-time adaptive stabilization of nonlinearly parametrized systems with multiple unknown control directions," *IEEE Trans. Syst., Man, Cybern. Syst.*, vol. 47, no. 7, pp. 1405–1414, Jul. 2017.

[50] X. Guo, H. Zhang, J. Sun, and Y. Zhou, "Preassigned time adaptive neural tracking control for stochastic nonlinear multiagent systems with deferred constraints," *IEEE Trans. Neural Netw. Learn. Syst.*, early access, Apr. 5, 2023, doi: 10.1109/TNNLS.2023.3262799.

[51] H. Zhou, S. Sui, and S. Tong, "Finite-time adaptive fuzzy prescribed performance formation control for high-order nonlinear multiagent systems based on event-triggered mechanism," *IEEE Trans. Fuzzy Syst.*, vol. 31, no. 4, pp. 1229–1239, Apr. 2023.

[52] X. Min, S. Baldi, and W. Yu, "Low-complexity control of nonholonomic mobile robots with formation constraints," in *Proc. IEEE 61st Conf. Decis. Control (CDC)*, 2022, pp. 4501–4506.